The substitution at residue 218 of the NS5 protein methyltransferase domain of Tembusu virus impairs viral replication and translation and may triggers RIG-I-like receptor signaling

Xuedong Wu [*,†], Yuhong Pan,[*,†] Juan Huang,[*,†] Shanzhi Huang,[*,†] Mingshu Wang,[*,†,‡] Shun Chen,[*,†,‡]
Mafeng Liu,[*,†,‡] Dekang Zhu,[*,†,‡] Xinxin Zhao,[*,†,‡] Ying Wu,[*,†,‡] Qiao Yang,[*,†,‡] Shaqiu Zhang,[*,†,‡]
Xumin Ou,[*,†,‡] Ling Zhang,[*,†] Yunya Liu,[*,†] Yanling Yu,[*,†] Qun Gao,[*,†] Sai Mao,[*,†] Di Sun,[*,†]
Bin Tian,[*,†] Zhongqiong Yin,[‡] Bo Jing,[‡] Anchun Cheng,[*,†,‡] and Renyong Jia[*,†,‡,1]

[*]Research Center of Avian Disease, College of Veterinary Medicine, Sichuan Agricultural University, Chengdu City,
Sichuan Province, 611130, China; [†]Institute of Preventive Veterinary Medicine, College of Veterinary Medicine,
Sichuan Agricultural University, Chengdu City, Sichuan Province, 611130, China; and [‡]Key Laboratory of Animal
Disease and Human Health of Sichuan Province, Chengdu City, Sichuan Province, 611130, China

ABSTRACT Flavivirus RNA cap-methylation plays an important role in viral infection, proliferation, and escape from innate immunity. The methyltransferase (**MTase**) of the flavivirus NS5 protein catalyzes viral RNA methylation. The E218 amino acid of the NS5 protein MTase domain is one of the active sites of flavivirus methyltransferase. In flaviviruses, the E218A mutation abolished 2'-O methylation activity and significantly reduced N-7 methylation activity. Tembusu virus (**TMUV**, genus *Flavivirus*) was a pathogen that caused neurological symptoms in ducklings and decreased egg production in laying ducks. In this study, we focused on a comprehensive understanding of the effects of the E218A mutation on TMUV characteristics and the host immune response. E218A mutation reduced TMUV replication and proliferation, but did not affect viral adsorption and entry. Based on a TMUV replicon system, we found that the E218A mutation impaired viral translation. In addition, E218A mutant virus might be more readily recognized by RIG-I-like receptors to activate the corresponding antiviral immune signaling than WT virus. Together, our data suggest that the E218A mutation of TMUV MTase domain impairs viral replication and translation and may activates RIG-I-like receptor signaling, ultimately leading to a reduction in viral proliferation.

Key words: TMUV, MTase domain, replication, translation, RIG-I-like receptor signaling

INTRODUCTION

Tembusu virus (**TMUV**) is a new member of the genus *Flavivirus* in the family *Flaviviridae* that mainly causes neurological symptoms in ducklings and decreased egg production in laying ducks and has zoonotic potential (Liu et al., 2013; Tang et al., 2013b). TMUV was first isolated from *Culex tritaeniorhynchus* mosquitoes in Malaysia in 1955 (Zhang et al., 2017). It was not until 2010 that the first outbreak of egg drop syndrome and neuroinflammation caused by TMUV in duck farms of southeast China attracted the attention of researchers, which has developed into one of the major pathogens in China duck farming, affecting the duck farming industry and causing huge economic losses (Cao et al., 2011). Studies have shown that TMUV can infect a wide variety of avian species, such as chickens (Liu et al., 2012a), geese (Huang et al., 2013; Ti et al., 2015), sparrows (Tang et al., 2013a), and pigeons, and replicates efficiently in a wide range of mammalian cells and mosquito cells (Yu et al., 2018). Although no human disease has been reported due to TMUV, antibodies against TMUV were detected in more than 70% of serum samples from duck industry workers, and about 50% of oral swab samples were positive for TMUV (Tang et al., 2013b). Recent study has reported that some people without the history of contact with ducks displayed high neutralizing antibody titers to TMUV (Pulmanausahakul et al., 2021). The host spectrum of the virus is expanding and there is a potential threat to public health, requiring strict biosecurity measures or polyvalent vaccines to control its spread.

Similar to other flaviviruses, including Japanese Encephalitis virus (**JEV**) and West Nile virus (**WNV**), TMUV has an approximately 11-kb single-stranded positive-sense RNA genome with a 5' type I cap structure (Zhu et al., 2015). The genome encodes a unique large precursor polyprotein that is cleaved by viral and host proteases into three structural proteins (capsid [C], premembrane [prM], and envelope [E]) and seven non-structural proteins (NS1, NS2A, NS2B, NS3, NS4A, NS4B, and NS5) (Liu et al., 2012b; Bai et al., 2013). The structural proteins mainly participate in receptor binding, membrane fusion, and virion assembly, while NS proteins are involved in viral RNA replication and innate immune evasion (Wang et al., 2016; Wu et al., 2019; Hu et al., 2021).

Flavivirus infection of host cells is a multistep and continuous process (Cruz-Oliveira et al., 2015; Yang et al., 2017). The first step of the life cycle is virus adsorption and entry. Flaviviruses enter cells through the receptor-mediated endocytosis at low pH and induce fusion with the endosome membrane. Then, flaviviruses release and translate their genomic RNA in the endoplasmic reticulum (**ER**). Viral RNA replication occurs in the virus-induced replication complex (**RC**) within a vesicle composed of endoplasmic reticulum (Gillespie et al., 2010; Garcia-Blanco et al., 2016). Following RNA synthesis, the nascent positive-strand RNA is capped and methylated by NS5 methyltransferase (**MTase**) to form a type I cap structure at the 5' end. The newly copied mature positive-stranded RNAs and the translated structural proteins are assembled in the lumen of the ER into immature virions, in which prM/E heterodimers form trimeric spikes with icosahedral symmetry (Klema et al., 2015; Mohd Ropidi et al., 2020). Subsequently, the prM protein is processed to mature M by host furin protease during the transit through the Golgi network. The immature noninfectious virions become mature infectious viruses and are released by exocytosis.

The TMUV NS5 protein, similar to that of other flaviviruses, is a highly structurally conserved enzyme protein with diverse functions. The C-terminus of NS5 protein contains an RNA-dependent RNA polymerase (**RdRp**) domain that synthesizes viral RNA by de novo synthesis (Ackermann and Padmanabhan, 2001; Calmels et al., 2017). The N-terminus of NS5 protein contains a MTase domain that catalyzes N-7 and 2'-O methylations in the formation of the 5'-end cap of the genome (Ray et al., 2006; Dong et al., 2014). The N-7 and 2'-O methylation processes of flaviviruses have been extensively studied (Zhou et al., 2007; Dong et al., 2010; Bradrick, 2017). Four conserved sites in the MTase domain of flavivirus NS5 protein constitute a catalytic tetrad (K61-D146-K182-E218) that plays an important regulatory role in N-7 and 2'-O methylations (Zhou et al., 2007). Previous studies have shown that the K61-D146-K182-E218 catalytic tetrad of flavivirus is essential for 2'-O methylation, while N-7 methylation requires only D146 (Wu et al., 2021). The cap structure of flavivirus plays an important role in virus cap-dependent translation and immune escape. Therefore, K-D-K-E catalytic

tetrad may regulate viral translation and host immune response. Previous studies have shown that human and mouse coronavirus mutants lacking 2'-O MTase activity induced higher expression of type I interferon (**IFN**) that was dependent on the cytoplasmic RNA sensor MDA5 (Züst et al., 2011). 2'-O methylation of the viral RNA evades host restriction of IFIT family members (Daffis et al., 2010). It has also been shown that yellow fever virus (**YFV**) used 2'-O methylation to suppress type I IFN induction by impairing RIG-I recognition (Schuberth-Wagner et al., 2015). In addition, Dengue virus (**DENV**) 2'-O MTase mutants are highly attenuated and immunogenic in mice and macaques (Züst et al., 2013), and JEV E218A mutant is highly attenuated in mice due to enhanced sensitivity to IFN and IFITs (Li et al., 2013). These RNA viruses lacking 2'-O MTase activity all showed some degree of attenuation in virulence or proliferation, but the causes were different. So how does TMUV lacking 2'-O MTase activity affects the biological characteristics of the virus and the host immune response? To explore this problem, we studied the proliferation, biological characteristics and effect on the host immune response of the E218A mutant virus. We found that the E218A mutation reduced TMUV proliferation by inhibiting viral replication and translation and possibly triggering host RIG-I-like receptor signaling.

MATERIALS AND METHODS

Cells and Viruses

Baby hamster kidney (**BHK-21**) cells were cultured in DMEM supplemented with 10% fetal bovine serum (**FBS**) at 37°C with 5% CO_2. Duck embryo fibroblast (**DEF**) cells isolated from 9-day-old healthy duck embryo were cultured in DMEM supplemented with 10% new-born calf serum (**NBCS**) at 37°C with 5% CO_2. The wild-type (**WT**) and E218A mutant viruses were rescued by our laboratory through the TMUV reverse genetics system (Wu et al., 2021).

Growth Curves of Recombinant TMUV

Growth curves of recombinant TMUV in DEF cells were analyzed. Briefly, cells were seeded into 12-well plates and then infected with 0.01 MOI WT and E218A viruses. After 1 h of incubation, the inoculum was removed, and DMEM containing 2% NBCS was added to the plates. Culture supernatant and cells were harvested at 24, 36, 60 h post-infection (**hpi**). The culture supernatant was used to determine the viral titer by the Fluorescence Formative Unit (**FFU**) assays. Total RNA was extracted from cells using RNAiso Plus (TaKaRa, Da lian, China), and the number of genome-containing particles was determined by absolute quantitative PCR (**qPCR**) that detected E gene according to the TB Green Premix Ex Taq II (TaKaRa) instructions.

RNA Extraction and Quantitative Reverse Transcription PCR

Total RNA was isolated from cells using RNAiso Plus (TaKaRa) and then reversely transcribed into cDNA using PrimeScript RT reagent Kit with gDNA Eraser (TaKaRa). The mRNA levels of cytokines and viral RNA copies were determined by qPCR following the TB Green Premix Ex Taq II (TaKaRa) instructions. The cycle threshold (**ct**) values were normalized with the mRNA level of the housekeeping gene GAPDH. The qPCR primers were listed in Table 1.

Virus Adsorption and Entry Assay

For the virus adsorption assay, DEF cells were infected with 0.01 MOI of WT or E218A virus at 4°C for 1 h. At this temperature, virus could bind to the cell surface without entry. At 1 hpi, cells were washed with precooled PBS three times to remove unbound viruses. Total RNA was extracted from cells to quantify viral RNA binding to the cell membrane by absolute qPCR

that detected E gene. Further incubation at 37°C initialized viral entry. After 1 h of incubation at 37°C, cells were thoroughly washed with PBS and alkaline high-salt solution to remove viruses on the cell surface. The alkaline high-salt solution can wash away viruses that has not been endocytosed on the cell surface (Yang et al., 2017). Total RNA was extracted from cells to quantify intracellular viral RNA by absolute qPCR that detected E gene.

Construction and Characterization of Mutant Replicon

E218A mutant replicon was constructed based on a negative control TMUV replicon with CMV promoter (pCMV-Replicon-NLuc-GDD/AAA; Wang et al., 2020) and an infectious cDNA clone of TMUV (pACYC-TMUV) (Chen et al., 2018). The replicon harbors a GDD-to-AAA mutation in the active site of the NS5 RNA polymerase that is conserved among flaviviruses. This mutation results in a loss of RNA polymerase

Table 1. Sequences of primers used in this study.

Primers	Sequences (5'-3')	Purpose
E218A-F	CGCGTAATTCAACGCATGCCATGTACTGGG	Mutagenesis
E218A-R	GGCATGCGTTGAATTACGCGAGAGTGGCAC	
EcoRv-F	AGACCTCCCTGTCTGGATATCGTACAAGGT CGCTGAAGCTGG	One-step cloning
SbfI-R	CATAACCCTAGCTGTTCCTGCAGGTGGTTC TGGGGCTTTGGTAT	
TMUV-E-qF	AATGGCTGTGGCTTGTTTGG	qPCR
TMUV-E-qR	GGGCGTTATCACGAATCTA	
TMUV-NS3-qF	TAAAGAGGGAGCATACTGG	
TMUV-NS3-qR	GCAGGGTCTGTGAAGTGA	
duRIG-I-qF	TGAGCTGCAAGGGAGACAAG	
duRIG-I-qR	TCCAATTCAGCTGACAGGGC	
duMDA5-qF	GCTACAGAAGATAGAAGTGTCA	
duMDA5-qR	CAGGATCAGATCTGGTTCAG	
duLGP2-qF	CGTTTACTTCTACTGCGTCAACTG	
duLGP2-qR	GTTGATGTTCACGTGGTGCAT	
duIFITM1-qF	CCCTGCTGCTCAACATCTTC	
duIFITM1-qR	GCTGATGGTGGAGCAGGTT	
duIRF1-qF	GAACTCCCTGCCTGACATCG	
duIRF1-qR	CTCTTGCTCCTGCTTCTTGCTT	
duIFNβ-qF	TCTACAGAGCCTTGCCTGCAT	
duIFNβ-qR	TGTCGGTGTCCAAAAGGATGT	
duIFIT5-qF	AAGCTACCTTCAAACGGGTA	
duIFIT5-qR	TCCTCCTTCAGCAAAGTCCA	
duIFI35-qF	GGATACAACAGGTGAAGAAC	
duIFI35-qR	ACTGGAGGGATTGGATTAG	
duMHC-I-qF	GAAGGAAGAGACTTCATTGCCTT	
duMHC-I-qR	TCTCCTCTCCAGTACGTCCTTCC	
duIFITM2-qF	TCTCTGGTCCCTCTTCAACGT	
duIFITM2-qR	GGCCTTGATGGAGAAGATGAG	
duIRF7-qF	CGCCACCCGCCTGAAGAAGT	
duIRF7-qR	CTGCCCGAAGCAGAGGAAGAT	
duSTAT1-qF	AAGGGAAACGGCTACATCAAG	
duSTAT1-qR	CATGGGCAGCAGATTTTCTG	
duTRIM25-qF	GAGAGGAGCTTTTGCAGTATGC	
duTRIM25-qR	GACAGACATCTTGGTGTATCTCTCAGA	
duVIPERIN-qF	TCCAGTTCTGCAAGGAGGAG	
duVIPERIN-qR	TTCTTGAACCACCGCTCTCT	
duPKR-qF	AATTCCTTGCCTTTTCATCCAA	
duPKR-qR	TTTGTTTTGTGCCATAGCTTGG	
duMX-qF	TGCTGTCCTTCATGACTTCG	
duMX-qR	GCTTTGCTGAGCCGATTAAC	
duGAPDH-qF	TGCTAAGCGTGTCATCATCT	
duGAPDH-qR	AGTGGTCATAAGACCCTCCA	

activity and blocks RNA synthesis of the replicon, generally serving as a negative control group (Xie et al., 2016; He et al., 2019). A subclone, pBlueScript-P4-6, containing the *EcoRv-SbfI* fragment of pACYC-TMUV (nucleotides 6229−8765 of the viral genome containing mutation site), was used to engineer mutation (pBlueScript-P4-6-E218A) using a *Fast* sitedirected Mutagenesis System (TransGen, China). The primers used for mutagenesis were listed in Table 1. PCR fragments containing the E218A substitution were amplified using pBlueScript-P4-6-E218A as template with primers listed in Table 1. Meanwhile, pCMV-Replicon-NLuc-GDD/AAA was digested by restriction enzymes *EcoRv* and *SbfI* (NEB). The amplified DNA fragments were fused with linearized pCMV-Replicon-NLuc-GDD/AAA by homologous recombination method to obtain pCMV-Replicon-NLuc-GDD/AAA-E218A. All plasmids were verified by DNA sequencing. To characterize the mutant replicon, BHK-21 cells seeded in 24-well plates were transfected with equal amounts of GDD/AAA and GDD/AAA+E218A replicons using Lipo3000. At 48 h post-transfection, cells were harvested, and a Nano-Glo Luciferase Assay System (Promega, Beijing, China) was used to detect luciferase activity of cells. At the same time, a parallel experiment was performed. Total RNA was extracted from cells using RNAiso Plus (TaKaRa). The copy number of replicon was quantified by absolute qPCR that detected NS3 gene.

Sample Preparation and Transcriptome Sequencing (RNA-Seq)

DEF cells preseeded into 6-well plates were infected with WT and E218A viruses at a MOI of 0.01. At 24 h post-infection, the cells were harvested quickly, frozen in liquid nitrogen for 5 min, and then stored at −80°C for later use. Total RNA was extracted from cells using the mirVana miRNA Isolation Kit (Ambion, Shanghai, China). The Agilent 2100 Bioanalyzer (Agilent Technologies, Beijing, China) was used to evaluate RNA integrity. The samples with RNA Integrity Number (**RIN**) ≥ 7 were subjected to the subsequent analysis. The TruSeq Stranded mRNA LTSample Prep Kit (Illumina, Shanghai, China) was used to construct cDNA Library. Then, these libraries were sequenced on the Illumina sequencing platform (HiSeqTM 2500 or Illumina HiSeq X Ten) and 125 bp/150 bp paired-end reads were generated. Finally, we obtained the original transcriptome data and submitted it to NCBI (Accession number: **PRJNA792214**).

Transcriptome Data Analysis

Bowtie2 (Langmead and Salzberg, 2012) and eXpress (Roberts and Pachter, 2013) were used to calculate FPKM (Kim et al., 2015) and read counts value of each transcript (protein coding). DEGs (*q*-value < 0.05 and fold Change > 2 or fold Change < 0.5) were identified using the DESeq functions estimateSizeFactors and nbinomTest. The expression patterns of transcripts were investigated by hierarchical clustering analysis of DEGs. GO enrichment and KEGG (Kanehisa et al., 2008) pathway enrichment analysis were respectively performed using R based on the hypergeometric distribution to determine the biological function or pathway affected by the differential transcript.

Dual-Luciferase Reporter Assay

DEF cells were cultured in 24-well plates to 80% confluence. Cells were co-transfected with 400 ng/well of IFNβ-Luc or IRF7-Luc and 100 ng/well of the Renilla luciferase-expressing construct TK-Luc. 24 h later, cells were infected with 0.01 MOI of WT and E218A viruses. After 24 h of infection, cells were harvested for luciferase activity detection following the Dual-Luciferase Reporter Assay System (Promega) instructions. The data are represented as the ratio of firefly to Renilla luciferase activity.

Statistical Analysis

The significance of the observed differences was assessed using unpaired Student's *t* test and two-way ANOVA test with GraphPad Prism 8.0. Differences were considered significant when *P*-values < 0.05. Data are expressed as mean ± standard deviation (**SD**).
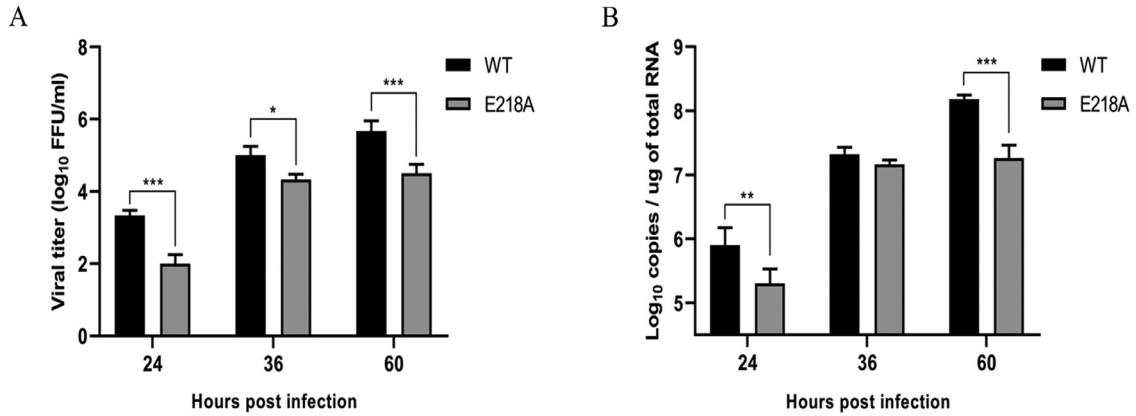
RESULTS

E218A Mutation Reduces the Replication and Proliferation of TMUV

To better evaluate the replication and proliferation of the mutant virus, we measured the growth curves of WT and E218A viruses in DEF cells. The E218A mutant group showed lower genomic copy numbers and viral titers in DEF cells than the WT group (Figures 1A and 1B). In detail, the viral titers of E218A virus showed approximately 1-log lower than that of WT virus at 24, 36, and 60 hpi (Figure 1A), and the copy numbers of E218A virus were also >0.5-log lower than that of WT virus at 24 and 60 hpi (Figure 1B). Overall, these results indicate that E218A mutation significantly reduces viral replication and proliferation.

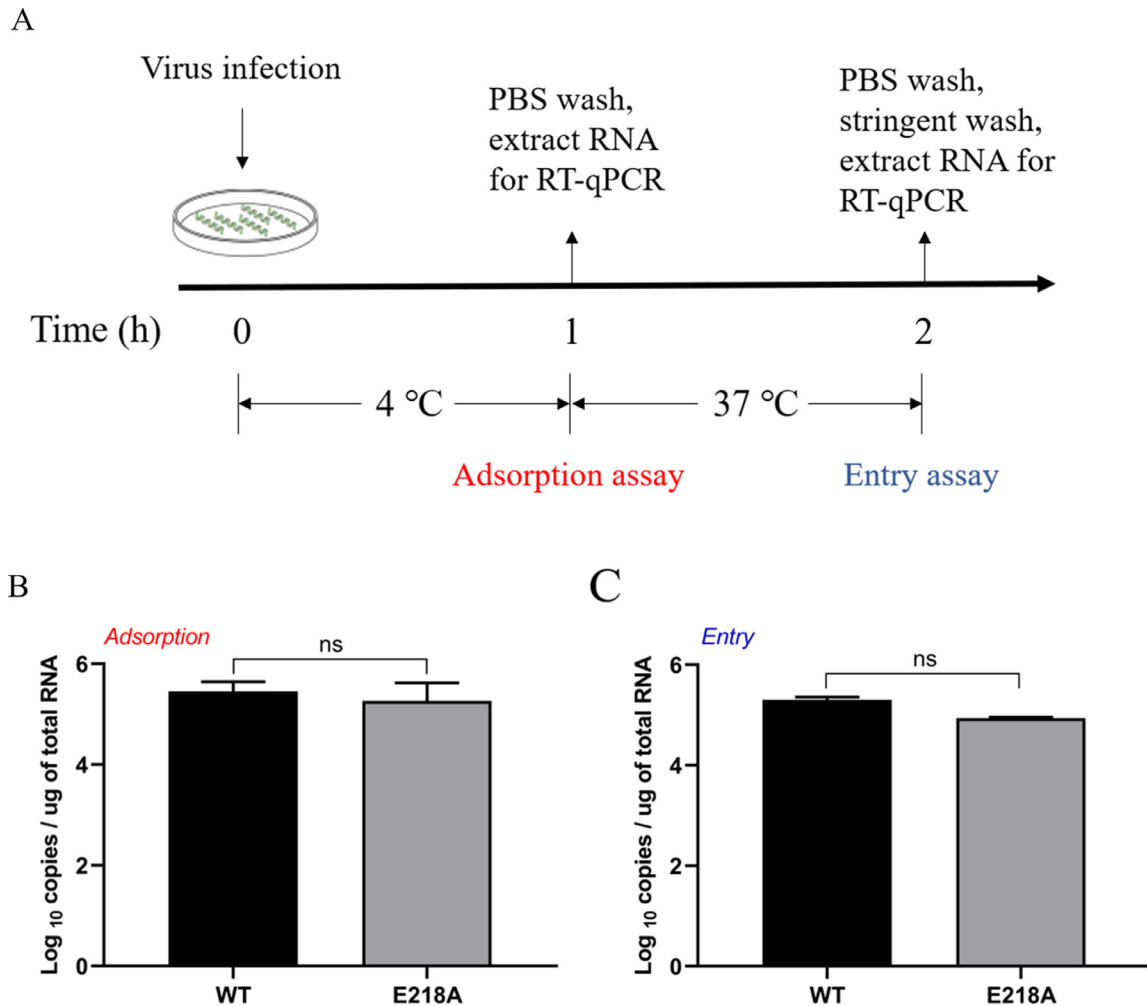### E218A Mutation Does Not Affect Viral Adsorption and Entry

A complete life cycle of flavivirus involves virion adsorption, entry, disassembly, genome replication, translation, and virus particle assembly, maturation and release. To investigate whether the E218A mutation affects viral adsorption and entry, we exploited absolute qPCR that detected E gene to measure the viral genomic RNA in the cells infected with WT and E218A viruses. Figure 2A depicts the experimental flowchart. First, DEF cells were infected with 0.01 MOI of WT and E218A

Figure 1. E218A mutation reduces the replication and proliferation of TMUV. (A, B) Growth kinetics of WT and E218A mutant viruses in DEF cells. Cells were infected with WT and E218A viruses at a MOI of 0.01. Viral titers (A) and RNA copy numbers (B) were measured at indicated times using fluorescence formative unit (FFU) and absolute qPCR assays. Each of these was conducted with three parallel replicates. Bars show means ± SDs. ***, $P < 0.001$; **, $P < 0.01$; *, $P < 0.05$ (two-way ANOVA).

viruses. For the viral adsorption assay (Hu et al., 2021), cells infected with the virus were incubated at 4°C for 1 h. At this temperature, viruses could bind to the cell surface without entry. The unbound viruses were removed by washing with precooled PBS. Then, we measured the amount of viral genomic RNA bound to the cell membrane. As shown in Figure 2B, E218A and WT viruses bound to DEF cells with equal efficiency, indicating that


Figure 2. E218A mutation does not affect viral adsorption and entry. (A) Schematic diagram for the viral adsorption and entry assay. (B, C) Determination of virus adsorption (B) and entry (C). DEF cells were infected with equal amounts of WT and E218A mutant viruses. At given time points, intracellular viral RNAs were quantified by absolute qPCR. Each of these was conducted with three parallel replicates. Bars show means ± SDs (Student's t test).

E218A mutation does not affect viral adsorption process. Further incubation at 37°C initialized virus entry. After 1 h of incubation, DEF cells were thoroughly washed with PBS and alkaline high-salt solution to remove viruses on the cell surface. The alkaline high-salt solution can wash away viruses that has not been endocytosed on the cell surface (Yang et al., 2017). Intracellular viral genomic RNA was quantified by qPCR. E218A virus showed no significant difference in entry ability from WT virus (Figure 2C). The result suggested that E218A mutation did not affect viral entry process. Taken together, these data demonstrate that E218A mutation does not interfere with viral adsorption and entry.

E218A Mutation Impairs Viral Translation

Since the MTase activity of NS5 protein is closely related to the formation of the 5'-end cap of the viral genome, which in turn is related to viral translation, we suspected whether the E218A mutation in the MTase region of NS5 protein affects the translation efficiency of the virus. To investigate the effect of the E218A mutation on viral translation, we developed a novel translation assay using a replicon that is incapable of RNA replication. The replicon harbors a GDD-to-AAA mutation in the active site of the NS5 RNA polymerase that is conserved among flaviviruses. This mutation results in a loss of RNA polymerase activity and blocks RNA synthesis of the replicon (Xie et al., 2016; He et al., 2019). As shown in Figure 3A, we introduced the E218A mutation into the GDD/AAA replicon to verify the effect of the E218A mutation on viral translation. The efficiency of viral translation was reflected by the Nano-Glo luciferase (**NLuc**) activity of replicon. The GDD/AAA+E218A replicon produced lower levels of NLuc activity than GDD/AAA replicon (Figure 3B), indicating that
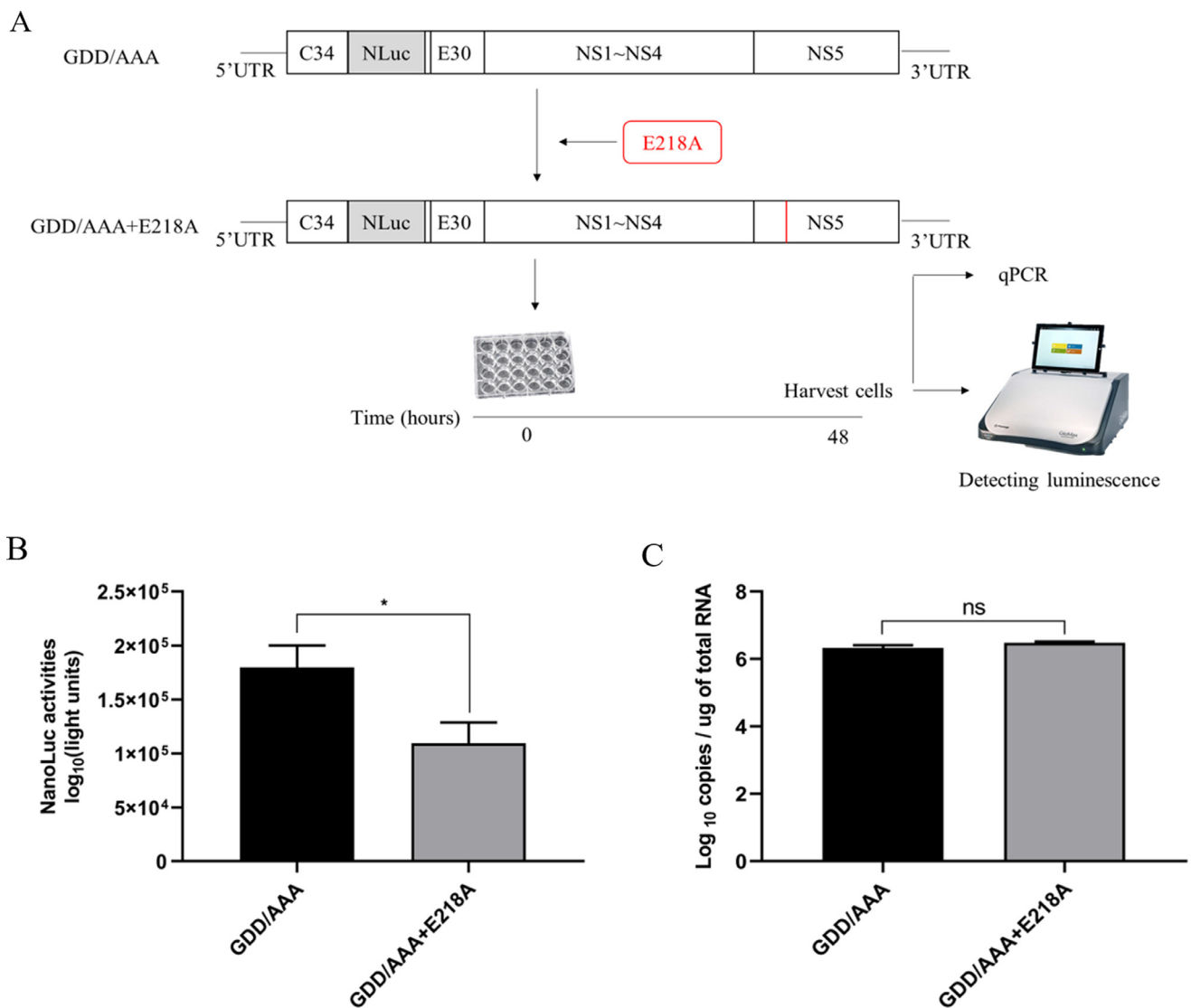
Figure 3. E218A mutation impairs viral translation. (A) Schematic diagram presentation and determination process of GDD/AAA and GDD/AAA+E218A replicons. The GDD/AAA+E218A replicon was constructed with GDD/AAA replicon as the backbone. BHK-21 cells were transfected with equal amounts of GDD/AAA and GDD/AAA+E218A replicons. At 48 h post-transfection, the cells were collected for NLuc activity and qPCR assays. (B) NLuc activity assay. Each of these was conducted with three parallel replicates. Bars show means ± SDs. (C) Copy numbers of replicons were determined by absolute qPCR. Each of these was conducted with three parallel replicates. Bars show means ± SDs. *, $P < 0.05$ (Student's t test).

Table 2. Sequencing data generated by an Illumina HiSeqTM 2500 sequencer.

Sample	Raw reads	Clean reads	Valid bases	Q30	Total mapped percentage
E218A1	47.85M	46.53M	94.50%	92.64%	81.77%
E218A2	48.91M	47.64M	94.77%	92.77%	82.15%
E218A3	43.32M	42.14M	94.69%	92.65%	82.02%
WT1	44.86M	43.69M	94.88%	92.75%	81.83%
WT2	49.93M	48.60M	94.20%	92.74%	82.15%
WT3	43.34M	42.14M	94.56%	92.66%	80.33%

the translation efficiency of GDD/AAA+E218A replicon was significantly reduced. To exclude the influence of replicon transfection differences, the copy number of replicon was detected by qPCR. The results showed that there was no statistically significant difference in copy number between GDD/AAA and GDD/AAA +E218A replicons (Figure 3C), indicating that the amounts of the 2 replicons transfected were almost equal. Overall, these data demonstrate that E218A mutation impairs viral translation.

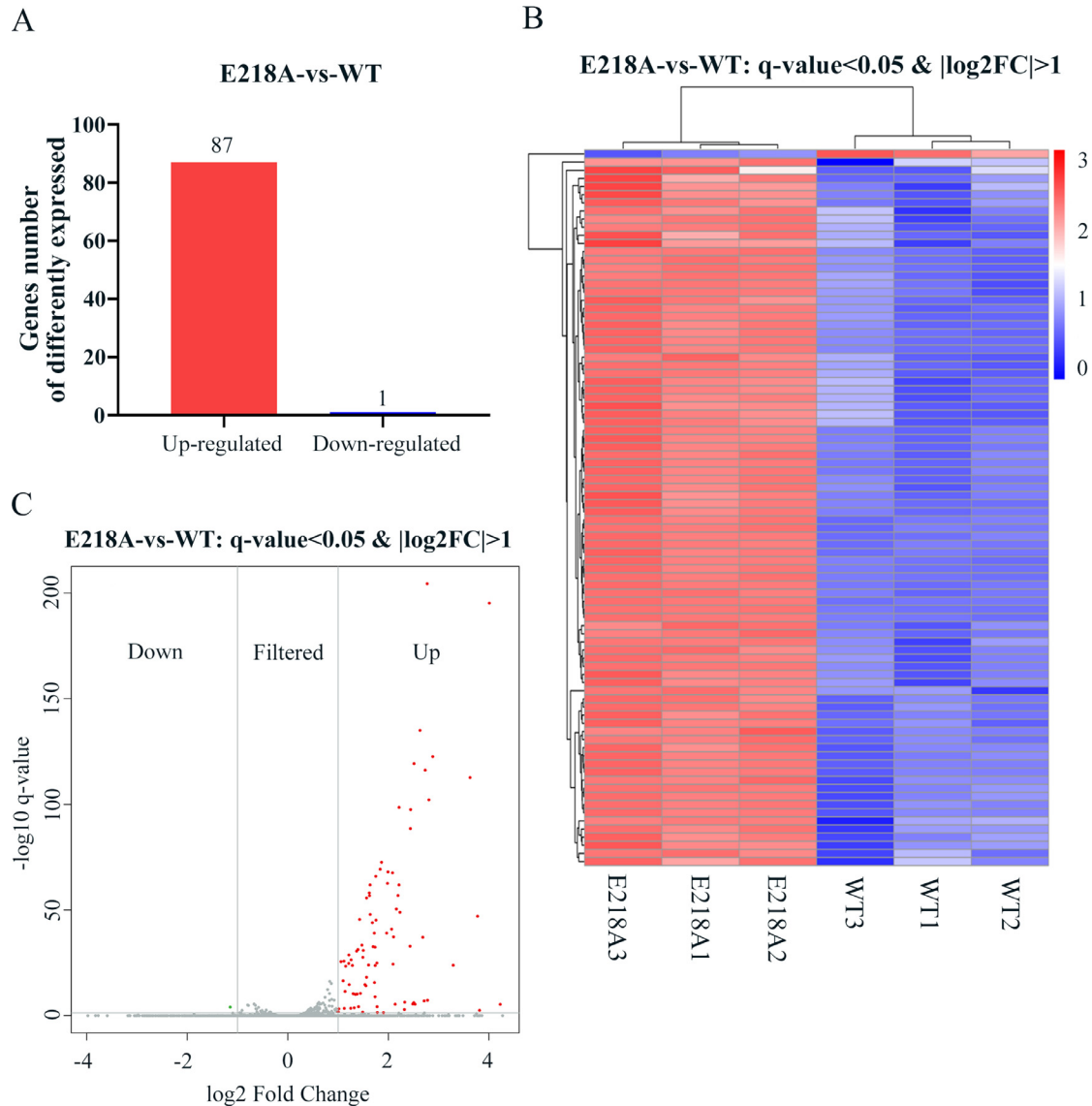## Identification of Differentially Expressed Genes

To deeply and comprehensively understand the effect of E218A mutation on the TMUV-induced innate immune response of the host, we determined transcriptional profiling of DEF cells infected with the WT or E218A virus. As shown in Table 2, the raw reads, clean reads, valid bases, Q30, and total mapped percentage of each sample were recorded for each library. An average of 6.58 Gbp clean bases was generated from each of the 6 samples. For all libraries, the valid bases, Q30, and total mapped ratio were >94%, >92%, and >80%, respectively. These results illustrated the high quality of the sequencing data and ensured their suitability for the next step of the analysis. A total of 88 differentially expressed genes (**DEGs**) was detected in E218A group compared to the WT group (q-value < 0.05 and fold change > 2 or fold Change < 0.5), composed of 87 upregulated genes and 1 down-regulated gene (Figure 4A). The expression of these DEGs in each sample and the significance of the differences were clearly visualized through the clustering of the samples by differential treatment and the construction of the volcano plot of DEGs (Figures 4B and 4C).

Expression Changes Mediated by E218A Mutant Virus

To comprehensively gain biological insight into the transcriptome data, the differentially expressed genes were analyzed for biological functions using Gene Ontology (**GO**) analysis. GO classification of the DEGs was annotated using 33 GO annotation, including 20 biological processes, 7 molecular functions and 6 cellular components (Figure 5A). For biological process annotation, the identified genes were mainly involved in cellular process (15.76%), biological regulation (13.65%), regulation

of biological process (13.18%), metabolic process (10.82%), response to stimulus (10.35%), and immune system process (5.88%) (Figure 5B). As shown in Figure 5C, the molecular function categories for regulated genes mainly included binding genes (58.06%), catalytic genes (29.03%), enzyme regulator genes (3.23%), molecular transduction genes (3.23%), and receptor regulatory genes (3.23%). Of note, TOP 30 GO enrichment analysis indicated that the functional classification of DEGs in biological processes was reflected in the defense response to virus, innate immune response, negative regulation of viral genome replication, and positive regulation of type I interferon signaling pathway (Figure 5D). All biological processes were mainly manifested in the significant activation of the host antiviral immune response, which is important for the host to resist viral infection. In addition, TOP 30 GO enrichment analysis indicated that the functional classification of DEGs in molecular function was mainly reflected in the doublestranded RNA binding, single-stranded RNA binding, STAT family protein binding, ubiquitin-like protein ligase binding, all of which were related to the activation of host innate immune response (Figure 5D). GO enrichment analysis showed that E218A mutant virus was more likely to activate the innate immune response than WT virus.

To further understand the functional changes regulated by E218A virus, KEGG enrichment analysis was conducted. KEGG pathway classification for up-regulated DEGs mainly included immune system (20%), signaling molecules and interaction (12%), cell growth and death (12%), transport and catabolism (12%), signal transduction (8%), and folding, sorting and degradation (8%) (Figure 6A). KEGG enrichment TOP 20 analysis found that 2 important immune signaling pathways were activated during E218A virus infection, namely RIG-I-like receptor signaling pathway and NOD-like receptor signaling pathway (Figure 6B). Notably, RIG-I-like receptor signaling pathway enriched more genes and acquired a higher enrichment score than NOD-like receptor signaling pathway (Figure 6B). By tracking the genes involved in KEGG enrichment TOP 20 (Figure 6C), we found that many genes associated with the RIG-I-like receptor signaling pathway were significantly up-regulated, such as RIG-I, MDA5, LGP2, TRIM25, and IRF7, as well as downstream antiviral genes STAT1, MX, PKR, and MHC-I. Overall, E218A TMUV may be more readily recognized by host immune receptors to activate antiviral immune response compared to WT virus.

A

E218A-vs-WT

B

E218A-vs-WT: q-value<0.05 & |log2FC|>1

C

E218A-vs-WT: q-value<0.05 & |log2FC|>1

Figure 4. Analysis of differentially expressed genes (DEGs) of the WT and E218A groups. (A) Statistic of differentially expressed genes. (B) A heatmap was used to classify the gene expression patterns. The x-axis represents the experimental conditions. (C) Volcano plot of DEGs between the WT and E218A groups. The y-axis indicates the negative logarithm of the q-value; the x-axis indicates the base 2 logarithm of fold change.

## The E218A Mutant Virus May Triggers RIG-I-Like Receptor Signaling

To verify the authenticity of the transcriptome data, representative 16 critical DEGs (these genes are associated with RIG-I-like receptor signaling) were subjected to RT-qPCR analysis. Compared with WT group, the expression of these genes was significantly up-regulated in the E218A group (Figure 7A). Importantly, the genes identified by RT-qPCR exhibited similar expression levels as those detected via transcriptomic analysis (Figure 7B). Furthermore, we determined the expression levels of IFNβ and IRF7, key genes involved in RIG-I-like receptor signaling, by a dual-luciferase reporter assay. As expected, E218A virus stimulated higher IFNβ and IRF7 production compared to WT virus (Figure 7C). Transcriptomic data, qPCR, and dual-luciferase reporter assay showed consistent results,

suggesting that the E218A mutant TMUV may induces RIG-I-like receptor signaling.

DISCUSSION

In this study, we measured the effect of a conserved amino acid E218 mutation of the methyltransferase region of TMUV NS5 protein on viral characteristics and host immune response, thus reflect the role of methylation at the 5' end of the viral genome in the virus life cycle and virus-host interaction. First, we found that E218A mutation did not affect viral adsorption and entry, but significantly impaired viral replication and translation. Furthermore, we found that E218A mutant TMUV may be more readily recognized by host immune receptors to activate antiviral immune responses.
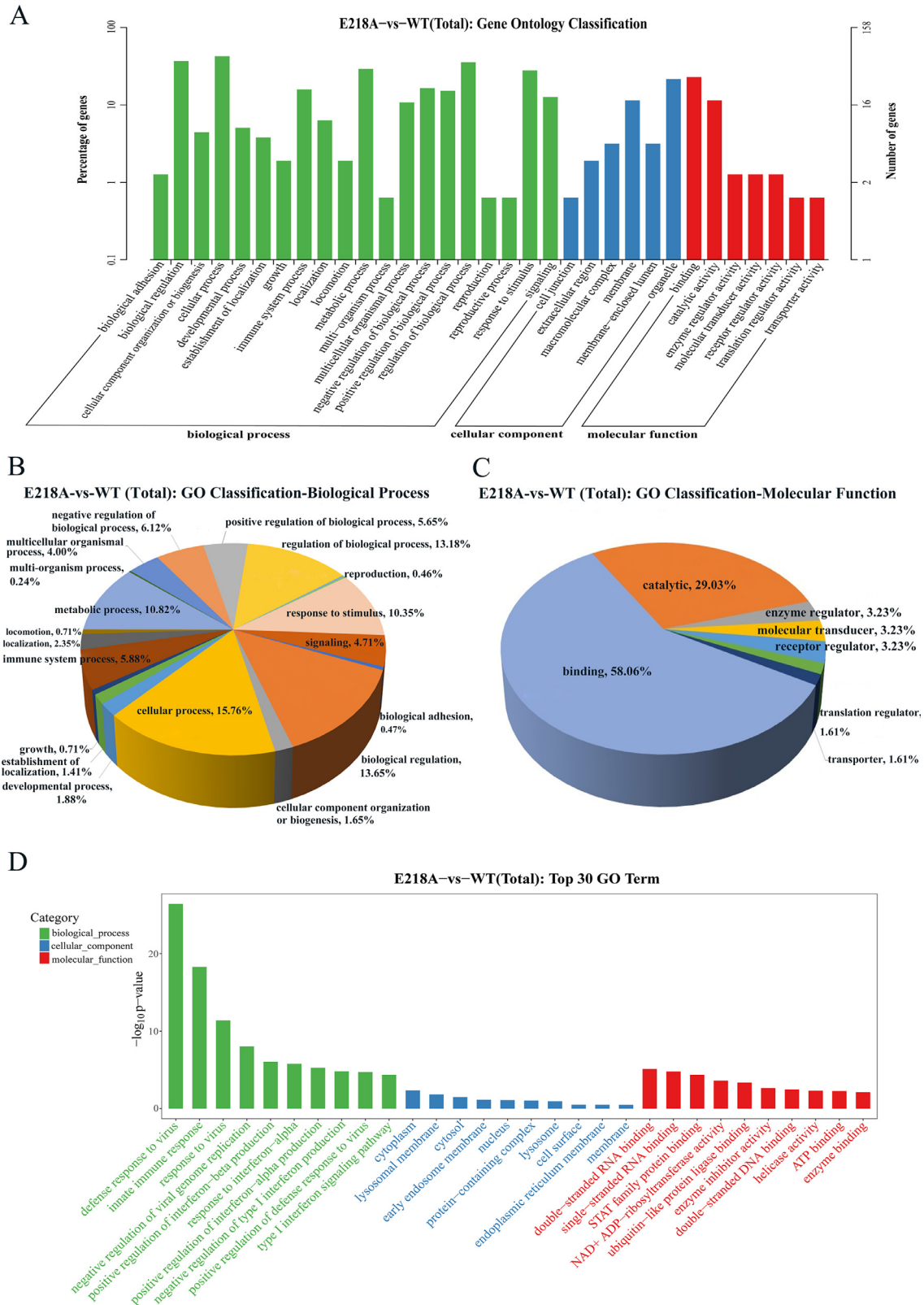
Figure 5. Gene ontology (GO) enrichment analysis of DEGs. (A) GO classification analysis of DEGs between the WT and E218A groups. The areas of the displayed histograms are proportional to the number of genes assigned to the term, and the colors correspond to the categories. (B, C) DEGs were classified according to biological processes (B) and molecular function (C). (D) TOP 30 GO enrichment analysis of DEGs. The colors correspond to the categories.

Ultimately, these effects lead to a reduction in the proliferation capacity of the E218A mutant.

5' end cap-methylation of the flavivirus genome is a necessary structural modification that ensures efficient expression of virus proteins (Zhao et al., 2015), blocks RNA degradation by 5'-3' exoribonucleases, and hides the viral genome from recognition by host immune receptors (Züst et al., 2011; Devarkar et al., 2016; Abbas
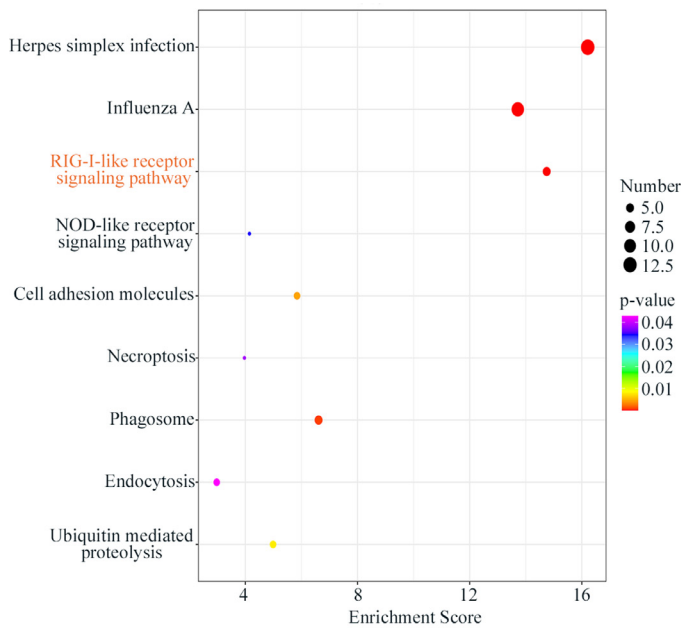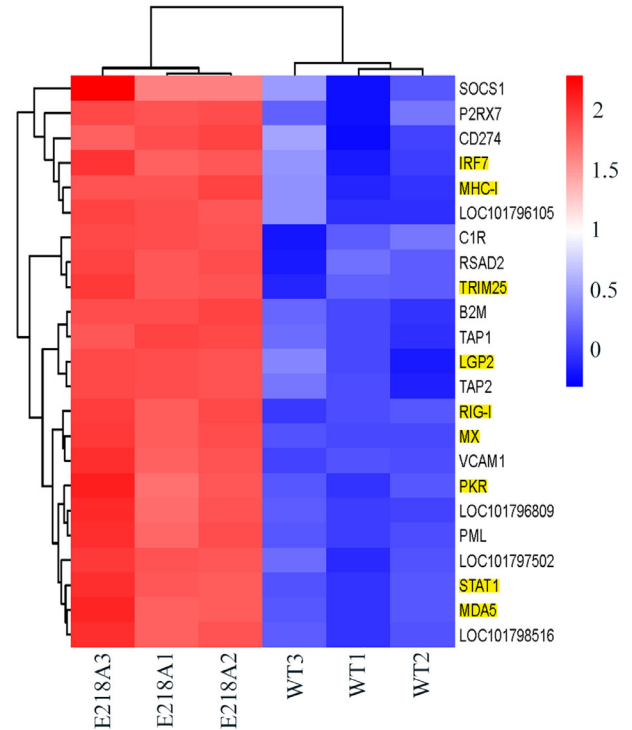
A

E218A-vs-WT (Up): KEGG Pathway Classification

B
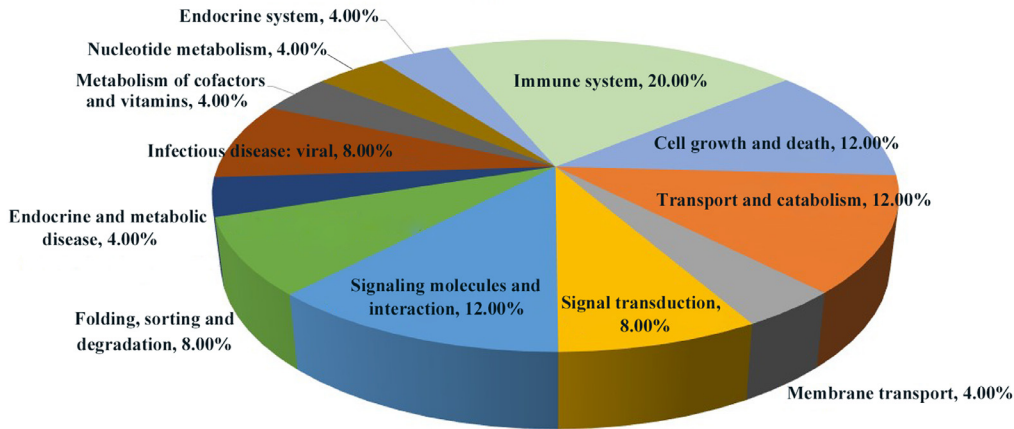
C

Figure 6. KEGG enrichment analysis of DEGs. (A) KEGG pathway classification of up-regulated DEGs. (B) KEGG enrichment TOP 20 analysis of up-regulated DEGs. (C) A heatmap of the genes involved in KEGG enrichment TOP 20 was constructed. The yellow highlighted genes are involved in RIG-I-like receptor signaling.

et al., 2017). E218A mutation abolishes 2'-O methylation of flavivirus genome and significantly reduces N-7 methylation activity (Dong et al., 2014). Incomplete methylation of the 5' cap may be the reason why TMUV E218A mutation impairs viral translation and induces antiviral innate immune response. In other flaviviruses, WNV-E218A is more sensitive to the antiviral actions of IFN-induced proteins with tetratricopeptide repeats (**IFIT**) genes (Daffis et al., 2010). YFV-E218A reached the same virus titers in RIG-I-deficient A549 cells as the

WT virus (Schuberth-Wagner et al., 2015). DENV1-E216A activated an earlier innate immune response in A549 cells, as compared to infection with WT DENV1, in this subset of genes including RIG-I and MDA5 (Chang et al., 2016). Human and mouse coronavirus mutants lacking 2'-O MTase activity induced higher expression of type I interferon that was dependent on the cytoplasmic RNA sensor MDA5 (Züst et al., 2011). The immune evasion of virus replication provides a reasonable explanation for the conservation of 2'-O
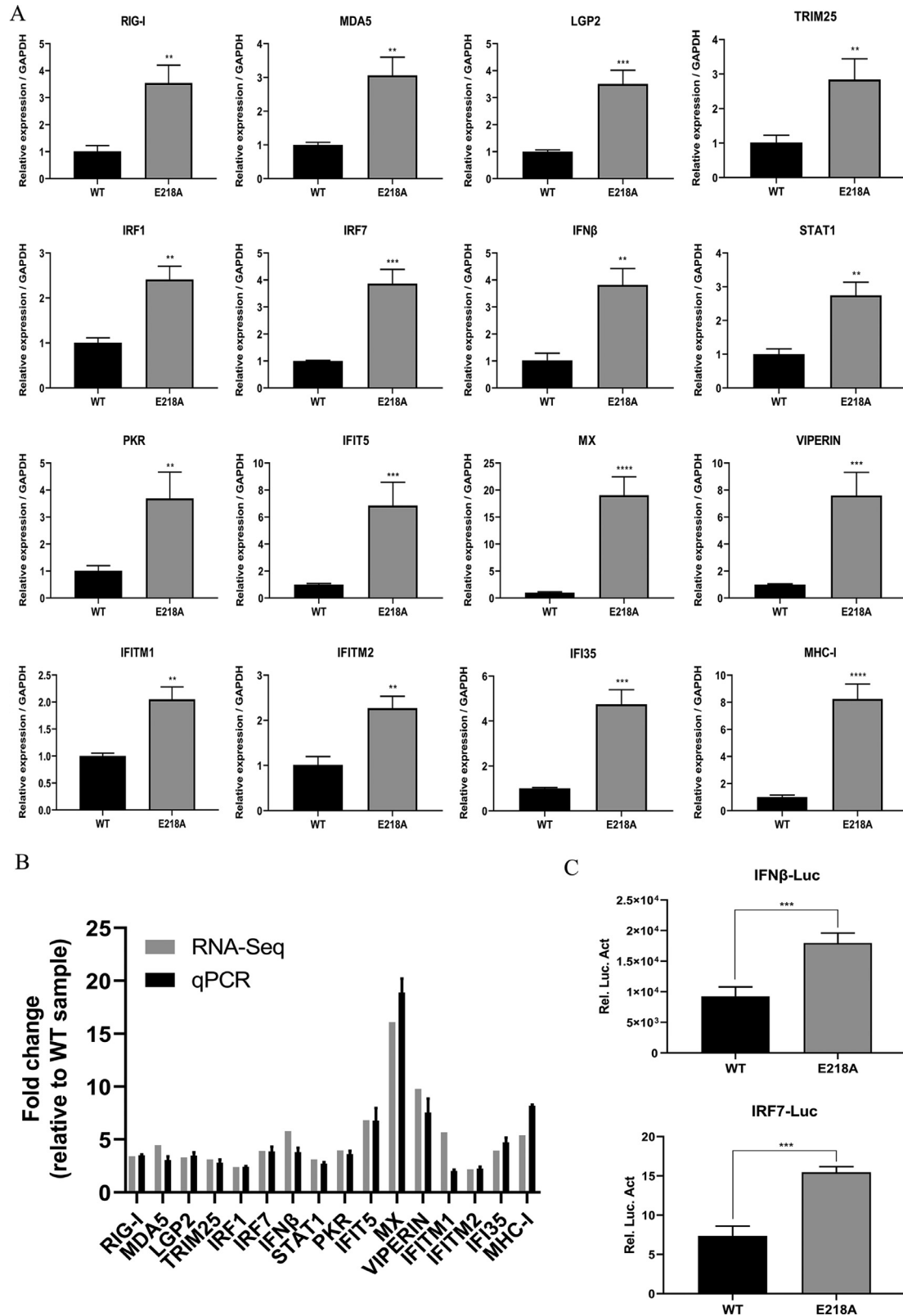
Figure 7. Validation of differentially expressed genes by RT-qPCR and dual-luciferase reporter assays. (A) Gene expression levels were measured by the $2^{-\Delta\Delta Ct}$ method with relative quantification. DEF cells were infected with WT or E218A virus (MOI = 0.01) and were harvested at 24 hpi. Intracellular mRNAs were extracted for RT-qPCR to measure the transcription levels of DEGs. Each of these was conducted with three parallel replicates. Bars show means ± SDs. ****, $P < 0.0001$; ***, $P < 0.001$; **, $P < 0.01$ (Student's t test). (B) The genes identified by RT-qPCR exhibited similar expression levels as those detected via transcriptomic analysis. (C) The productions of IFNβ and IRF-7 induced by WT and E218A viruses were determined by dual-luciferase reporter assay. DEF cells were co-transfected with 400 ng/well of IFNβ-Luc or IRF7-Luc and 100 ng/well of the Renilla luciferase-expressing construct TK-Luc. 24 h later, the cells were infected with 0.01 MOI of WT and E218A viruses. After 24 h of infection, cells were harvested for luciferase activity detection. Each of these was conducted with three parallel replicates. Bars show means ± SDs. ***, $P < 0.001$ (Student's t test).

methyltransferases in many RNA viruses that replicate in the cytoplasm of higher eukaryotes.

The translation mechanisms of flavivirus have been extensively studied, including cap-dependent and cap-independent translation mechanisms (Edgil et al., 2006). Cap-dependent translation mechanism is mainly mediated by m7G structure (Wang et al., 2020), which is modified by N-7 methylation. Decreased N-7 methylation activity may lead to translation inhibition of E218A mutant TMUV. There are very few studies on the correlation between flavivirus methylation and viral translation, most of which focus on viral genomic methylation and immune escape, and our study just makes up for this neglected link. However, our relevant research is superficial, and further research is needed to clarify the mechanism involved. Some studies have shown that murine IFIT1 inhibits replication of MTase-defective JEV or mouse hepatitis virus (**MHV**) by inhibiting mRNA translation through direct binding to 5' capped 2'-O unmethylated RNA (Habjan et al., 2013; Kimura et al., 2013). The specific and stable interaction between IFIT1 and Cap 0-mRNA may be the reason why it inhibits translation and thus impairs replication of specific viruses (Kumar et al., 2014). Human IFIT5 has comparable affinity for RNAs with the monophosphate, triphosphate, cap 0 at the 5'-end, excluding the higher eukaryotic mRNA cap (**cap I**) (Katibah et al., 2014). Although birds only have IFIT5, it is possible that IFIT5 binds to the 2'-O unmethylated RNA of the Tembusu virus to inhibit viral translation and thereby inhibit viral replication and proliferation. Transcriptome data analysis showed that the expression of IFIT5 was significantly up-regulated, which just indicated that IFIT5 might play a role in translation inhibition of E218A mutant virus. This precisely links the host innate immune response to viral translation. But further research is needed to identify this possibility.

MTase has become an attractive target for the development of live attenuated vaccine and antiviral drug. Previous studies have shown that DENV-E217A mutant was highly attenuated and immunogenic in mice and macaques (Züst et al., 2013). JEV-E218A mutant was attenuated and protected the mice against lethal challenge with virulent virus strains (Li et al., 2013). WNVs deficient in 2'-O methylation were attenuated and could protect mice from later wild-type virus challenge (Zhou et al., 2007). MHV deficient in N-7 MTase activity induced both humoral and cellular immune responses, which could protect mice against the challenge of a lethal-dose of MHV-A59 (Zhang et al., 2021). In addition, some adenine dinucleosides SAM analogs or nucleoside analogues selectively inhibit RNA virus methyltransferases (Chen et al., 2013; Ahmed-Belkacem et al., 2020). The combination of our study and previous studies provides a direction for the development of live attenuated vaccine and antiviral inhibitor against TMUV by targeting MTase.

In conclusion, our data suggest that the E218A mutation of TMUV MTase domain impairs viral replication and translation and may activates RIG-I-like receptor signaling, ultimately leading to a reduction in viral proliferation. This study provides scientific theoretical basis for further development of live attenuated vaccine and antiviral inhibitor against TMUV by targeting MTase.

DISCLOSURES

The authors declare that they have no conflict of interest.

REFERENCES

Abbas, Y. M., B. T. Laudenbach, S. Martínez-Montero, R. Cencic, M. Habjan, A. Pichlmair, M. J. Damha, J. Pelletier, and B. Nagar. 2017. Structure of human IFIT1 with capped RNA reveals adaptable mRNA binding and mechanisms for sensing N1 and N2 ribose 2′-O methylations. Proc. Nat. Acad. Sci. U.S.A. 114: E2106–E2115.

Ackermann, M., and R. Padmanabhan. 2001. De novo synthesis of RNA by the dengue virus RNA-dependent RNA polymerase exhibits temperature dependence at the initiation but not elongation phase. J. Biol. Chem. 276:39926–39937.

Ahmed-Belkacem, R., P. Sutto-Ortiz, M. Guiraud, B. Canard, J. J. Vasseur, E. Decroly, and F. Debart. 2020. Synthesis of adenine dinucleosides SAM analogs as specific inhibitors of SARS-CoV nsp14 RNA cap guanine-N7-methyltransferase. Eur. J. Med. Chem. 201:112557.

Bai, X., R. Lv, C. Liu, N. Qiu, Y. He, X. Yin, X. Li, M. Liu, and Y. Zhang. 2013. Molecular characterization of a duck Tembusu virus from China. Virus Genes 47:478–482.

Bradick, S. S. 2017. Causes and consequences of flavivirus RNA methylation. Front. Microbiol. 8:1–6.

Calmels, C., M. Ventura, C. Aknin, M. Métifiot, and M. L. Andreola. 2017. De novo RNA synthesis catalyzed by the Zika Virus RNA polymerase domain. Sci. Rep. 7:1–9.

Cao, Z., C. Zhang, Y. Liu, W. Ye, J. Han, G. Ma, D. Zhang, F. Xu, X. Gao, Y. Tang, S. Shi, C. Wan, C. Zhang, B. He, M. Yang, X. Lu, Y. Huang, Y. Diao, X. Ma, and D. Zhang. 2011. Tembusu virus in ducks, China. Emerg. Infect. Dis. 17:1873–1875.

Chang, D. C., L. T. Hoang, A. N. Mohamed Naim, H. Dong, M. J. Schreiber, M. L. Hibberd, M. J. A. Tan, and P. Y. Shi. 2016. Evasion of early innate immune response by 2′-O-methylation of dengue genomic RNA. Virology 499:259–266.

Chen, H., L. Liu, S. A. Jones, N. Banavali, J. Kass, Z. Li, J. Zhang, L. D. Kramer, A. K. Ghosh, and H. Li. 2013. Selective inhibition of the West Nile virus methyltransferase by nucleoside analogs. Antiviral Res. 97:232–239.

Chen, S., Y. He, R. Zhang, P. Liu, C. Yang, Z. Wu, J. Zhang, M. Wang, R. Jia, D. Zhu, M. Liu, Q. Yang, Y. Wu, and A. Cheng. 2018. Establishment of a reverse genetics system for duck Tembusu virus to study virulence and screen antiviral genes. Antiviral Res. 157:120–127.

Cruz-Oliveira, C., J. M. Freire, T. M. Conceição, L. M. Higa, M. A. R. B. Castanho, and A. T. Da Poian. 2015. Receptors and routes of dengue virus entry into the host cells. FEMS Microbiol. Rev. 39:155–170.

Daffis, S., K. J. Szretter, J. Schriewer, J. Li, S. Youn, J. Errett, T. Y. Lin, S. Schneller, R. Zust, H. Dong, V. Thiel, G. C. Sen, V. Fensterl, W. B. Klimstra, T. C. Pierson, R. M. Buller, M. Gale Jr, P. Y. Shi, and M. S. Diamond. 2010. 2′-O methylation

of the viral mRNA cap evades host restriction by IFIT family members. Nature 468:452–456.

Devarkar, S. C., C. Wang, M. T. Miller, A. Ramanathan, F. Jiang, A. G. Khan, S. S. Patel, and J. Marcotrigiano. 2016. Structural basis for m7G recognition and 2′-O-methyl discrimination in capped RNAs by the innate immune receptor RIG-I. Proc. Nat. Acad. Sci. U.S.A. 113:596–601.

Dong, H., D. C. Chang, X. Xie, Y. X. Toh, K. Y. Chung, G. Zou, J. Lescar, S. P. Lim, and P. Y. Shi. 2010. Biochemical and genetic characterization of dmddmddengue virus methyltransferase. Virology 405:568–578.

Dong, H., K. Fink, R. Züst, S. P. Lim, C. F. Qin, and P. Y. Shi. 2014. Flavivirus RNA methylation. J. Gen. Virol. 95:763–778.

Edgil, D., C. Polacek, and E. Harris. 2006. Dengue virus utilizes a novel strategy for translation initiation when cap-dependent translation is inhibited. J. Virol. 80:2976–2986.

Garcia-Blanco, M. A., S. G. Vasudevan, S. S. Bradrick, and C. Nicchitta. 2016. Flavivirus RNA transactions from viral entry to genome replication. Antiviral Res. 134:244–249.

Gillespie, L. K., A. Hoenen, G. Morgan, and J. M. Mackenzie. 2010. The endoplasmic reticulum provides the membrane platform for biogenesis of the flavivirus replication complex. J. Virol. 84:10438–10447.

Habjan, M., P. Hubel, L. Lacerda, C. Benda, C. Holze, C. H. Eberl, A. Mann, E. Kindler, C. Gil-Cruz, J. Ziebuhr, V. Thiel, and A. Pichlmair. 2013. Sequestration by IFIT1 impairs translation of 2′O-unmethylated capped RNA. PLoS Pathog. 9:e1003663.

He, Y., P. Liu, T. Wang, Y. Wu, X. Lin, M. Wang, R. Jia, D. Zhu, M. Liu, X. Zhao, Q. Yang, Y. Wu, S. Zhang, Y. Liu, L. Zhang, Y. Yu, L. Pan, S. Chen, and A. Cheng. 2019. Genetically stable reporter virus, subgenomic replicon and packaging system of duck Tembusu virus based on a reverse genetics system. Virology 533:86–92.

Hu, T., Z. Wu, S. Wu, M. Wang, R. Jia, D. Zhu, M. Liu, X. Zhao, Q. Yang, Y. Wu, S. Zhang, J. Huang, S. Mao, X. Ou, Q. Gao, D. Sun, Y. Liu, L. Zhang, Y. L. Yu, S. Chen, and A. Cheng. 2021. Substitutions at loop regions of TMUV E protein domain III differentially impair viral entry and assembly. Front. Microbiol. 12:1–12.

Huang, X., K. Han, D. Zhao, Y. Liu, J. Zhang, H. Niu, K. Zhang, J. Zhu, D. Wu, L. Gao, and Y. Li. 2013. Identification and molecular characterization of a novel flavivirus isolated from geese in China. Res. Vet. Sci. 94:774–780.

Kanehisa, M., M. Araki, S. Goto, M. Hattori, M. Hirakawa, M. Itoh, T. Katayama, S. Kawashima, S. Okuda, T. Tokimatsu, and Y. Yamanishi. 2008. KEGG for linking genomes to life and the environment. Nucleic Acids Res. 36:480–484.

Katibah, G. E., Y. Qin, D. J. Sidote, J. Yao, A. M. Lambowitz, and K. Collins. 2014. Broad and adaptable RNA structure recognition by the human interferon-induced tetratricopeptide repeat protein IFIT5. Proc. Nat. Acad. Sci. U.S.A. 111:12025–12030.

Kim, D., B. Langmead, and S. L. Salzberg. 2015. HISAT: a fast spliced aligner with low memory requirements. Nat. Methods 12:357–360.

Kimura, T., H. Katoh, H. Kayama, H. Saiga, M. Okuyama, T. Okamoto, E. Umemoto, Y. Matsuura, M. Yamamoto, and K. Takeda. 2013. Ifit1 inhibits Japanese Encephalitis virus replication through binding to 5' capped 2'-O unmethylated RNA. J. Virol. 87:9997–10003.

Klema, V. J., R. Padmanabhan, and K. H. Choi. 2015. Flaviviral replication complex: coordination between RNA synthesis and 5'-RNA capping. Viruses 7:4640–4656.

Kumar, P., T. R. Sweeney, M. A. Skabkin, O. V. Skabkina, C. U. T. Hellen, and T. V. Pestova. 2014. Inhibition of translation by IFIT family members is determined by their ability to interact selectively with the 5'-terminal regions of cap0-, cap1- and 5'ppp-mRNAs. Nucleic Acids Res. 42:3228–3245.

Langmead, B., and S. L. Salzberg. 2012. Fast gapped-read alignment with Bowtie 2. Nat. Methods 9:357–359.

Li, S.-H., H. Dong, X.-F. Li, X. Xie, H. Zhao, Y.-Q. Deng, X.-Y. Wang, Q. Ye, S.-Y. Zhu, H.-J. Wang, B. Zhang, Q.-B. Leng, R. Zuest, E.-D. Qin, C.-F. Qin, and P.-Y. Shi. 2013. Rational design of a flavivirus vaccine by abolishing viral RNA 2'-O methylation. J. Virol. 87:5812–5819.

Liu, M., S. Chen, Y. Chen, C. Liu, S. Chen, X. Yin, G. Li, and Y. Zhang. 2012a. Adapted tembusu-like virus in chickens and geese in China. J. Clin. Microbiol. 50:2807–2809.

Liu, M., C. Liu, G. Li, X. Li, X. Yin, Y. Chen, and Y. Zhang. 2012b. Complete genomic sequence of duck flavivirus from China. J. Virol. 86:3398–3399.

Liu, P. P., H. Lu, S. Li, Y. Wu, G. F. Gao, and J. L. Su. 2013. Duck egg drop syndrome virus: an emerging Tembusu-related flavivirus in China. Sci. Chin. Life Sci. 56:701–710.

Mohd Ropidi, M. I., A. S. Khazali, N. Nor Rashid, and R. Yusof. 2020. Endoplasmic reticulum: a focal point of Zika virus infection. J. Biomed. Sci. 27:1–13.

Pulmanausahakul, R., K. Ketsuwan, T. Jaimipuk, D. R. Smith, P. Auewarakul, and T. Songserm. 2021. Detection of antibodies to duck tembusu virus in human population with or without the history of contact with ducks. Transbound. Emerg. Dis. 00:1–4.

Ray, D., A. Shah, M. Tilgner, Y. Guo, Y. Zhao, H. Dong, T. S. Deas, Y. Zhou, H. Li, and P.-Y. Shi. 2006. West Nile virus 5'-Cap structure is formed by sequential guanine N-7 and ribose 2'-O methylations by nonstructural protein 5. J. Virol. 80:8362–8370.

Roberts, A., and L. Pachter. 2013. Streaming fragment assignment for real-time analysis of sequencing experiments. Nat. Methods 10:71–73.

Schuberth-Wagner, C., J. Ludwig, A. K. Bruder, A. M. Herzner, T. Zillinger, M. Goldeck, T. Schmidt, J. L. Schmid-Burgk, R. Kerber, S. Wolter, J. P. Stümpel, A. Roth, E. Bartok, C. Drosten, C. Coch, V. Hornung, W. Barchet, B. M. Kümmerer, G. Hartmann, and M. Schlee. 2015. A conserved histidine in the RNA sensor RIG-I controls immune tolerance to N1-2'-O-methylated self RNA. Immunity 43:41–51.

Tang, Y., Y. Diao, C. Yu, X. Gao, X. Ju, C. Xue, X. Liu, P. Ge, J. Qu, and D. Zhang. 2013a. Characterization of a tembusu virus isolated from naturally infected house sparrows (Passer domesticus) in northern China. Transbound. Emerg. Dis. 60:152–158.

Tang, Y., X. Gao, Y. Diao, Q. Feng, H. Chen, X. Liu, P. Ge, and C. Yu. 2013b. Tembusu virus in human, China. Transbound. Emerg. Dis. 60:193–196.

Ti, J., L. Zhang, Z. Li, D. Zhao, Y. Zhang, F. Li, and Y. Diao. 2015. Effect of age and inoculation route on the infection of duck Tembusu virus in Goslings. Vet. Microbiol. 181:190–197.

Wang, J., C.-Q. Lei, Y. Ji, H. Zhou, Y. Ren, Q. Peng, Y. Zeng, Y. Jia, J. Ge, B. Zhong, Y. Li, J. Wei, H.-B. Shu, and Q. Zhu. 2016. Duck Tembusu virus nonstructural protein 1 antagonizes IFN-β signaling pathways by targeting VISA. J. Immunol. 197:4704–4713.

Wang, T., A. Merits, Y. Wu, M. Wang, R. Jia, D. Zhu, M. Liu, X. Zhao, Q. Yang, Y. Wu, S. Zhang, Y. Liu, L. Zhang, Y. Yu, L. Pan, S. Chen, and A. Cheng. 2020. cis -Acting sequences and secondary structures in untranslated regions of duck tembusu virus RNA are important for cap-independent translation and viral proliferation. J. Virol. 94:e00906–e00920.

Wu, X., Y. Zhang, M. Wang, S. Chen, M. Liu, D. Zhu, X. Zhao, Y. Wu, Q. Yang, S. Zhang, J. Huang, X. Ou, L. Zhang, Y. Liu, Y. Yu, Q. Gao, S. Mao, D. Sun, B. Tian, Z. Yin, B. Jing, A. Cheng, and R. Jia. 2021. Methyltransferase-deficient avian flaviviruses are attenuated due to suppression of viral RNA translation and induction of a higher innate immunity. Front. Immunol. 12:751688.

Wu, Z., W. Zhang, Y. Wu, T. Wang, S. Wu, M. Wang, R. Jia, D. Zhu, M. Liu, X. Zhao, Q. Yang, Y. Wu, S. Zhang, Y. Liu, L. Zhang, Y. Yu, L. Pan, A. Merits, S. Chen, and A. Cheng. 2019. Binding of the duck tembusu virus protease to STING is mediated by NS2B and is crucial for STING cleavage and for impaired induction of IFN-β. J. Immunol. 203:3374–3385.

Xie, X., J. Zou, C. Shan, Y. Yang, D. B. Kum, K. Dallmeier, J. Neyts, and P. Y. Shi. 2016. Zika virus replicons for drug discovery. EBioMedicine 12:156–160.

Yang, Y., C. Shan, J. Zou, A. E. Muruato, D. N. Bruno, B. de Almeida Medeiros Daniele, P. F. C. Vasconcelos, S. L. Rossi, S. C. Weaver, X. Xie, and P. Y. Shi. 2017. A cDNA clone-launched platform for high-yield production of inactivated Zika vaccine. EBioMedicine 17:145–156.

Yu, G., Y. Lin, Y. Tang, and Y. Diao. 2018. Evolution of tembusu virus in ducks, chickens, geese, sparrows, and mosquitoes in Northern China. Viruses 10:1–9.

Zhang, W., S. Chen, S. Mahalingam, M. Wang, and A. Cheng. 2017. An updated review of avian-origin tembusu virus: a newly emerging avian flavivirus. J. Gen. Virol. 98:2413–2420.

Zhang, Z., Q. Liu, Y. Sun, J. Li, J. Liu, R. Pan, L. Cao, X. Chen, Y. Li, Y. Zhang, K. Xu, D. Guo, L. Zhou, K. Lan, and Y. Chen. 2021. Live attenuated coronavirus vaccines deficient in N7-Methyltransferase activity induce both humoral and cellular immune responses in mice. Emerg. Microb. Infect. 10:1626–1637.

Zhao, Y., T. S. Soh, S. P. Lim, K. Y. Chung, K. Swaminathan, S. G. Vasudevan, P. Y. Shi, J. Lescar, and D. Luo. 2015. Molecular basis for specific viral RNA recognition and 2'-O-ribose methylation by the dengue virus nonstructural protein 5 (NS5). Proc. Nat. Acad. Sci. U.S.A. 112:14834–14839.

Zhou, Y., D. Ray, Y. Zhao, H. Dong, S. Ren, Z. Li, Y. Guo, K. A. Bernard, P.-Y. Shi, and H. Li. 2007. Structure and function of flavivirus NS5 methyltransferase. J. Virol. 81:3891–3903.

Zhu, K., J. Huang, R. Jia, B. Zhang, M. Wang, D. Zhu, S. Chen, M. Liu, Z. Yin, and A. Cheng. 2015. Identification and molecular characterization of a novel duck Tembusu virus isolate from Southwest China. Arch. Virol 160:2781–2790.

Züst, R., L. Cervantes-Barragan, M. Habjan, R. Maier, B. W. Neuman, J. Ziebuhr, K. J. Szretter, S. C. Baker, W. Barchet, M. S. Diamond, S. G. Siddell, B. Ludewig, and V. Thiel. 2011. Ribose 2'-O-methylation provides a molecular signature for the distinction of self and non-self mRNA dependent on the RNA sensor Mda5. Nat. Immunol. 12:137–143.

Züst, R., H. Dong, X. F. Li, D. C. Chang, B. Zhang, T. Balakrishnan, Y. X. Toh, T. Jiang, S. H. Li, Y. Q. Deng, B. R. Ellis, E. M. Ellis, M. Poidinger, F. Zolezzi, C. F. Qin, P. Y. Shi, and K. Fink. 2013. Rational design of a live attenuated dengue vaccine: 2'-O-methyltransferase mutants are highly attenuated and immunogenic in mice and macaques. PLoS Pathog. 9:e1003521.